A biosensor assay for studying ligand-membrane receptor interactions: Binding of antibodies and HIV-1 Env to chemokine receptors

Trevor L. Hoffman*, Gabriela Canziani†, Li Jia‡, Joseph Rucker§¶, and Robert W. Doms*¶

Departments of *Pathology and Lab Medicine, †Medicine, and ‡Biochemistry and Biophysics, University of Pennsylvania, Philadelphia, PA 19104; and §Department of Chemistry, Villanova University, Villanova, PA 19085

Edited by Peter S. Kim, Massachusetts Institute of Technology, Cambridge, MA, and approved July 21, 2000 (received for review June 14, 2000)

The HIV envelope (Env) protein mediates entry into cells by binding CD4 and an appropriate coreceptor, which triggers structural changes in Env that lead to fusion between the viral and cellular membranes. The major HIV-1 coreceptors are the seven transmembrane domain chemokine receptors CCR5 and CXCR4. The type of coreceptor used by a virus strain is an important determinant of viral tropism and pathogenesis, and virus-receptor interactions can be therapeutic targets. However, Envs from many virus strains interact with CXCR4 and CCR5 with low affinity such that direct study of this important interaction is difficult if not impossible using standard cell-surface binding techniques. We have developed an approach that makes it possible to study ligand binding to membrane proteins, including Env–coreceptor interactions, using an optical biosensor. CCR5, CXCR4, and other membrane proteins were incorporated into retrovirus particles, which were purified and attached to the biosensor surface. Binding of conformationally sensitive antibodies as well as Env to these receptors was readily detected. The equilibrium dissociation constant for the interaction between an Env derived from the prototype HIV-1 strain IIIB for CXCR4 was approximately 500 nM, explaining the difficulty in measuring this interaction using standard equilibrium binding techniques. Retroviral pseudotypes represent easily produced, stable, homogenous structures that can be used to present a wide array of single and multiple membrane-spanning proteins in a native lipid environment for biosensor studies, thus avoiding the need for detergent solubilization, purification, and reconstitution. The approach should have general applicability and can be used to correlate Env–receptor binding constants to viral tropism and pathogenesis.

Ligand interactions with membrane proteins are responsible for a multitude of cell adhesion, signaling, and regulatory events. This diversity of functions makes membrane proteins, such as seven transmembrane domain (7TM) receptors, important drug targets. Proteins that span the membrane multiple times present a unique set of challenges for ligand binding studies because they require a lipid environment to maintain native structure. Whereas detergent conditions can occasionally be found that allow native structure to be maintained in solution, this is an empirical and frequently time-consuming process. As a result, ligand binding studies involving 7TM and many other membrane proteins typically involve using whole cells or vesicles derived from cell membranes, where the protein of interest is a minor component.

Interactions between the HIV-1 envelope (Env) protein and its receptors underscore both the strengths and weaknesses of cell-surface binding assays. HIV-1 Env mediates virus entry by sequentially binding to CD4 and a coreceptor, with these interactions triggering conformational changes in Env that lead to membrane fusion (1). R5 virus strains that are responsible for virus transmission use the 7TM chemokine receptor CCR5 in conjunction with CD4 to enter cells, X4 virus strains that tend to evolve years after infection use the related CXCR4 receptor, and intermediate dual-tropic R5X4 virus strains can use both receptors. Binding of the soluble gp120 subunit of Env to CD4 is readily detected, and gp120 proteins from some R5 virus strains bind to CCR5 with high affinity (2, 3). However, direct binding of X4 gp120 proteins to CXCR4 has been difficult to measure, as has binding of R5X4 gp120 proteins to either CXCR4 or CCR5 (4–6). Interactions between Env and alternative coreceptors such as CCR3 and STRL33 also cannot be measured using standard binding techniques (5). As virus–receptor interactions can be the targets of neutralizing antibodies and small molecule inhibitors (reviewed in ref. 1), improved assays to measure these binding events are needed.

An approach that in principle would make it possible to monitor low affinity but functionally important Env–coreceptor interactions would be to use optical biosensors, a class of analytical instruments that detect interactions between molecules in real-time. The most commonly used optical biosensors (Biacore, Uppsala, Sweden) are based on surface plasmon resonance, which measures changes in refractive index at the sensor surface (7, 8). With this technique, one protein is tethered to the biosensor surface, and changes in refractive index that occur upon exposure to its binding partner are monitored. However, a general method for attaching intact membrane proteins to this instrument does not exist. In this paper, we describe the development of a novel technique to study ligand binding to both topologically simple and complex transmembrane proteins using the optical biosensor by presenting these proteins on the surface of retroviral particles. We found that a number of type 1 and 7TM domain chemokine receptors can be incorporated into virions, which can be easily purified and attached to the biosensor surface. Binding of antibodies and HIV-1 gp120 to these receptors exhibited appropriate specificity, and structural integrity of the receptors was maintained. The use of these retroviral pseudotypes in the optical biosensor eliminates the need to purify and reconstitute membrane proteins for ligand binding studies and provides a general experimental technique to characterize functionally important interactions with membrane proteins that would otherwise not be possible with standard equilibrium binding assays.

Materials and Methods

Proteins. HIV-1 HXBc2 and 8x gp120 were produced and purified by lectin chromatography (9). The anti-gp120 mAb 17b was provided by J. Robinson (Tulane University, New Orleans) (10,

This paper was submitted directly (Track II) to the PNAS office.

Abbreviations: 7TM, seven transmembrane domain; MLV, murine leukemia virus; RU, response unit.

¶To whom reprint requests may be addressed. E-mail: rucker@chem.vill.edu or doms@mail.med.upenn.edu.

The publication costs of this article were defrayed in part by page charge payment. This article must therefore be hereby marked "*advertisement*" in accordance with 18 U.S.C. §1734 solely to indicate this fact.

Article published online before print: *Proc. Natl. Acad. Sci. USA*, 10.1073/pnas.190274097. Article and publication date are at www.pnas.org/cgi/doi/10.1073/pnas.190274097

11). mAbs CTC8 and #549 to CCR5 and mAbs R&D#8 and R&D#16 were provided by M. Tsang (R & D Systems) (12). mAbs 4G10 and 7C11.1 to CXCR4 were a gift of C. Broder (Uniformed Services University of the Health Sciences, Bethesda) (13), anti-CXCR4 mAb 12G5 was provided by J. Hoxie (University of Pennsylvania, Philadelphia) (14), and anti-CCR5 mAb 2D7 was from Research Diagnostics (Flanders, NJ). ALX40–4C, a specific peptide inhibitor of CXCR4, was provided by Allelix (Salt Lake City). (15). The murine antibody 9E10 was used for detection of the myc epitope (16). Chick collapsin-1 containing a histidine tail was purified via nickel column chromatography (17).

Pseudotype Production, Purification, and Characterization. Murine leukemia virus (MLV) pseudotypes were produced by calcium phosphate-mediated transfection of 293T cells in 225-cm^2 flasks with a 3:1 ratio of receptor plasmid to pCGP, which encodes the MLV gag and pol genes. Four hours posttransfection, fresh media supplemented with 10 mM *n*-butyric acid was added to increase protein expression. 48 h posttransfection, supernatant was harvested, and cell debris was removed by low speed centrifugation and 0.45 μm filtration. The supernatant was pelleted for 90 min in an SW28 rotor at 28,000 RPM through 20% sucrose/PBS and resuspended overnight in PBS. A second ultracentrifugation step through 20% sucrose/PBS was performed in an SW40 rotor at 40,000 RPM for 45 min, and the pellet was resuspended in 100 μl of 10 mM Hepes, pH 7.4. The pseudotypes were either stored at 4°C or aliquoted and frozen at −20°C. MLV pseudotypes were analyzed for MLV gag and receptor expression by SDS-PAGE and Western blot. Pseudotypes were also analyzed by equilibrium density gradient ultracentrifugation using a 15–45% sucrose gradient at 35,000 RPM for 16 h in a SW40 rotor. Particles were also examined by negative stain electron microscopy on carbon films after staining with uranyl acetate.

Attachment of Pseudotypes to Biosensor Surfaces. All attachments were performed in PBS running buffer using Bia2000 or BiaX optical biosensors (Biacore, Uppsala, Sweden) at 25°C. Pseudotypes were attached to a gold surface derivatized with a carboxylated alkane thiol (Biacore C1 chip) or a short carboxydextran matrix (Biacore F1 chip) following a 10-min activation of surface carboxyl groups using a 1:1 mixture of 1-ethyl-3-(3-dimethylaminopropyl)carbodiimide hydrochloride (EDC) (1 M) and *N*-hydroxysuccinimide (0.25 M) at 5 μl/min. Pseudotypes that had been mixed 1:1 with 0.1 M sodium acetate, pH 5.5, were injected manually until the desired level of response units (RU), usually between 2,000 and 6,000 RU, had been reached. Following attachment, the remaining surface carboxyl groups were quenched with 35 μl of 1 M ethanolamine, pH 8.5, at 5 μl/min.

Binding Experiments. Binding experiments were performed in DMEM with 0.1% Pluronic F127 (Sigma) or PBS without surfactants at 30 μl/min and at 25°C unless otherwise noted. Importantly, every binding experiment performed included a reference surface containing an equivalent RU amount of MLV particles made with pCDNA3 or other receptor as a negative control. Analyte was removed following each binding interaction using duplicate 20-μl pulses of regeneration solution at 100 μl/min. Regeneration conditions varied for each ligand/analyte pair and were optimized empirically to remove all bound protein and maintain surface activity using various combinations of pH 5 (0.15 M oxalic acid/0.15 M H_3PO_4/0.15 M formic acid/0.15 M malonic acid, pH 5), pH 9 (0.2 M ethanolamine/0.2 M Na_3PO_4/0.2 M glycine/0.2 M piperazine, pH 9), 1 M NaCl, 1 M $MgCl_2$, and chaotropic (0.46 M KCSN/1.83 M $MgCl_2$/0.92 M urea/1.83 M guanidine·HCl) solutions (18). Data analysis and fitting was performed with BIAEVALUATION 3.0 software.

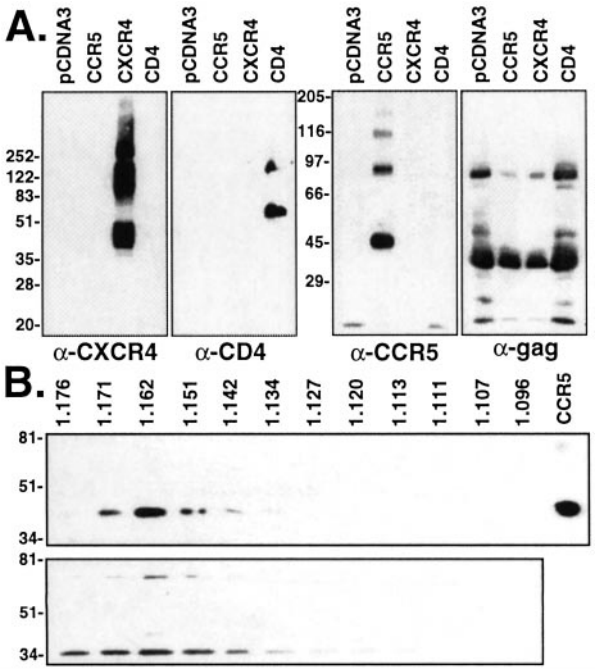

Fig. 1. Western blots of MLV pseudotypes. (*A*) MLV particles were produced by cotransfection of 293T cells with plasmids expressing MLV gag and either the indicated receptor constructs or an empty pCDNA3 vector (MLV–pCDNA3). Purified MLV–pCDNA3, MLV–CCR5, MLV–CXCR4, and MLV–CD4 particles were analyzed by Western blot using antibodies against the various receptors and the MLV gag protein as indicated. (*B*) Fractions from an equilibrium density gradient containing MLV–CCR5 were analyzed by SDS-PAGE and Western blot using antibodies to CCR5 (*Upper*) and MLV-gag (*Lower*). Densities of each fraction are indicated (in g/ml), and a CCR5 standard was run in the far right lane to control for expression.

Results

Receptor Incorporation and Characterization of MLV Particles. Retroviruses can nonspecifically incorporate cell-surface membrane proteins into their lipid envelope as they bud from the plasma membrane (19–21). To determine whether retroviral pseudotypes could be used to present membrane proteins in their native conformations for optical biosensor studies, we transiently coexpressed different transmembrane proteins with the structural proteins necessary to generate MLV particles in 293T cells. The media were collected, and virus particles were purified by ultracentrifugation and analyzed for the presence of the viral core protein (gag) and the desired membrane protein. The type I membrane protein CD4 and the 7TM chemokine receptors CCR5 and CXCR4 were incorporated into virus particles at readily detectable levels (Fig. 1*A*). The virus particles were judged pure by equilibrium gradient centrifugation (Fig. 1*B*) and negative stain electron microscopy, which revealed a homogenous population of vesicular structures with an average diameter of 105 ± 29 nm (data not shown).

Immobilization of MLV Particles to Biosensor Surfaces. To perform binding studies using the purified receptor-bearing MLV particles, it was necessary to capture the virions to a derivatized gold surface suitable for use in the optical biosensor. A number of sensor surfaces are available from Biacore, each with different surface properties. We used a standard coupling chemistry technique in which sensor surface carboxyl groups are activated with *N*-hydroxysuccinimide/EDC, permitting subsequent formation of covalent bonds with primary amines on the virion surface. The most frequently used sensor chip (CM5) contains a ~100 nM dextran hydrogel derivatized with carboxyl groups

(22). Because viral particles are likely to be negatively charged and surface plasmon resonance decays exponentially as a function of distance from the biosensor surface, we used a carboxymethylated surface that lacks a dextran matrix (Biacore C1 chip). We were able to reliably attach 4,000–6,000 RU of virus particles to the C1 chip but had difficulty obtaining robust attachment of MLV particles onto the CM5 surface. However, suitable attachment (4,000–6,000 RU) could be obtained on a sensor chip with a shorter dextran surface (Biacore F1 chip). We found that the optimal pH for attachment of the pseudotypes was 5.5 for all surfaces and receptors. Following attachment, reductions in baseline were not observed with time or repeated regeneration, indicating that the particles were irreversibly linked to the sensor surface.

Antibody Binding Studies to MLV Particles Containing Chemokine Receptors. Equivalent amounts of MLV particles containing CCR5 (MLV–CCR5), CXCR4 (MLV–CXCR4), or no receptor (MLV–pCDNA3) were attached to the biosensor surface, and binding of specific antibodies was measured. The anti-CXCR4 antibody 12G5, which recognizes a conformational epitope in CXCR4 (4, 23), bound to MLV–CXCR4 and did not bind to MLV–CCR5 or MLV–pCDNA3 (Fig. 2*A*). The anti-CCR5 antibody CTC8, which recognizes a linear epitope on the N terminus of CCR5 (12), bound to MLV–CCR5 and did not bind to MLV–pCDNA3 or MLV–CXCR4 (Fig. 2*B*). When PBS was washed across the sensor surface following injection of the antibodies, a typical dissociation curve was observed (arrows in Fig. 2 *A* and *B*). Similar results were obtained with CCR5 mAbs #549 and 2D7 and CXCR4 mAbs 4G10, R&D#8, and R&D#16 to both linear and conformational epitopes (not shown). Mouse IgG and BSA showed minimal binding to any of the MLV particles on the F1 or C1 chips.

For retroviral pseudotypes to be successful vehicles for presenting membrane proteins on a biosensor surface, they have to withstand multiple regeneration cycles in which bound analytes are removed without damaging either the particles or the receptors they contain. In this way, multiple binding experiments can be performed with a single surface, a prerequisite for the accurate determination of binding constants. We found that a brief pulse with a regeneration mixture containing an equal proportion of pH5 and chaotropic solutions (18) efficiently removed 12G5 from MLV–CXCR4 particles, returning the signal to baseline (Fig. 2*A*, bars). A single injection of this regeneration buffer was also sufficient to remove CTC8 from MLV–CCR5 particles, again returning the signal to baseline (Fig. 2*B*, bar). Similar results were obtained with other CCR5 and CXCR4 antibodies. The reproducibility and stability of the MLV particles to multiple binding and regeneration cycles is shown in Fig. 2*C*. Overlay plots from six sequential binding reactions on the same biosensor surface performed with 12G5 were virtually identical. Results with CTC8 were similar (not shown). These results indicate that the regeneration conditions removed antibody from the surface without damaging the MLV particles or altering receptor conformation. In fact, binding experiments could be performed over the course of several days before significant decreases in the binding capacity of the MLV particles was observed on a given sensor chip (not shown). In addition, MLV particles could be stored at −20°C for at least several weeks before attachment and use in biosensor experiments.

As an additional specificity control, we tested the ability of ALX40–4C, a small peptide inhibitor of CXCR4, to block 12G5 binding to MLV–CXCR4 particles (15). As shown in Fig. 2*D*, inclusion of ALX40–4C in the running buffer eliminated 12G5 binding to MLV–CXCR4 at a concentration (4 μM) similar to that needed to inhibit HIV-1 infection (15). Furthermore, ALX40–4C could be washed out and full binding of 12G5 to MLV–CXCR4 restored (Fig. 2*D*). The ability of CTC8 to bind MLV–CCR5 was unaffected by the presence of ALX40–4C (not shown). The reversible ability of ALX40–4C to specifically prevent 12G5 binding to MLV–CXCR4 confirms the specificity of the pseudotype system.

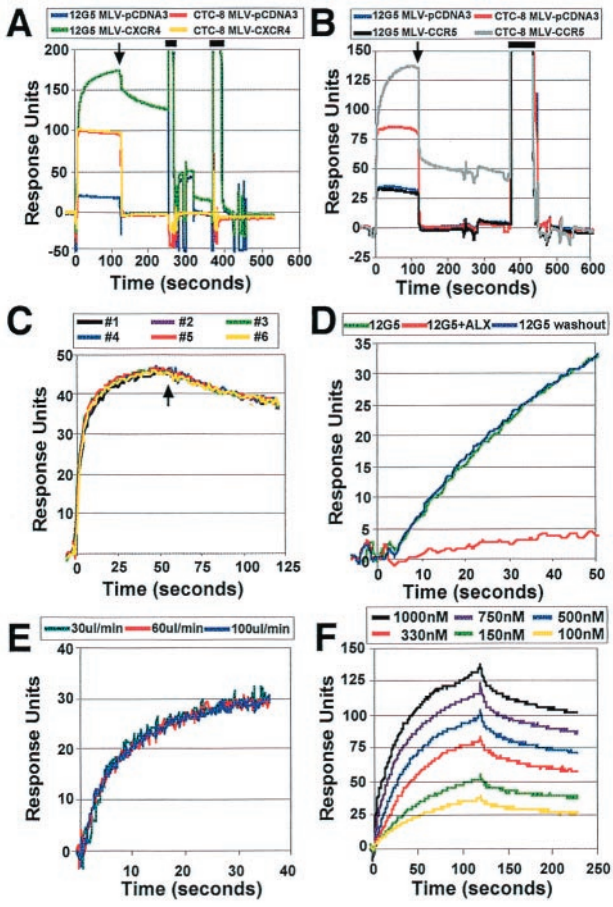

Fig. 2. Antibody binding to chemokine receptor pseudotypes. (*A*) Equivalent amounts of MLV–CXCR4 and MLV–pCDNA3 were attached to a Biacore F1 chip. Binding of 333 nM 12G5 and 666 nM CTC8 to MLV–CXCR4 and MLV–pCDNA3 is shown. Binding was measured for 120 s before washing with PBS running buffer for an additional 120 s to measure dissociation (indicated by arrow). Regeneration pulses are indicated by bars. Instrument noise between the regeneration pulses is due to changes in flow rate and the injections of the regeneration buffer, which lead to immediate shifts in the signal baseline. The slower changes in signal reflect binding of proteins to the sensor surface. (*B*) Equivalent amounts of MLV–CCR5 and MLV–pCDNA3 were attached to a Biacore F1 chip, and the binding of 400 nM CTC8 or 800 nM 12G5 to MLV–CCR5 and MLV–pCDNA3 is shown. A single regeneration pulse (bar) was used to strip bound antibody. (*C*) The data from six sequential injections of 166 nM 12G5 to MLV–pCDNA3 and MLV–CXCR4 are overlayed. In all cases, and in all subsequent figures, the sensorgrams show subtracted data, in which the signal obtained from the control surface is subtracted from the signal obtained from the surface bearing receptor-positive particles. Binding was measured for 60 s. Regeneration conditions were similar to those used in *A*. (*D*) Subtracted data from the binding of 5 nM 12G5 to MLV–CXCR4 and MLV–pCDNA3 is shown in green. After regeneration, binding in the presence of the CXCR4 inhibitor ALX40–4C (at 4 μM) is shown in red, whereas binding of the antibody following washout of the inhibitor is shown in blue. (*E*) Subtracted data for serial injections of 111 nM 12G5 to MLV–CXCR4 and MLV–pCDNA3 at different flow rates are shown. Regeneration conditions were similar to those used in *A*. (*F*) Subtracted data from binding of serial dilutions of CTC8 to MLV–CCR5 and MLV–pCDNA3 are shown.

Having shown that antibody binding to chemokine receptors on MLV pseudotypes was specific and highly reproducible, a

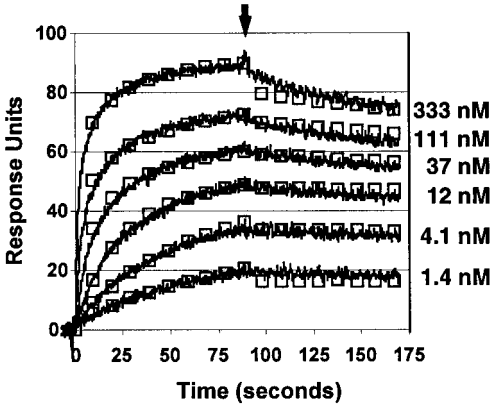

Fig. 3. Bivalent binding of 12G5 to MLV–CXCR4. Sensorgrams of 12G5 binding to MLV–CXCR4 are shown at different mAb concentrations, with the signals obtained from 12G5 binding to the MLV–pCDNA3 surface being subtracted. Binding was measured for 90 s and dissociation for 80 s before regeneration. Global analysis of the data using Biaevaluation 3.0 software was performed, and the boxes indicate the best fit of the data to a bimolecular interaction.

series of experiments was performed to assess the kinetic constants of these interactions. Binding of 12G5 to CXCR4 particles at different flow rates ensured that ligand binding to the MLV particles was not diffusion-limited (Fig. 2*E*). Results were similar for CTC8 and other anti-CCR5 and anti-CXCR4 antibodies (not shown). Next, the binding of the mAbs CTC8 and 12G5 to the chemokine receptors CCR5 and CXCR4 was measured using a range of antibody concentrations (Figs. 2*F* and 3), and the data were analyzed using BIAEVALUATION 3.0 software. Analysis of the binding curves for 12G5 indicated that the data were consistent with a bivalent interaction (χ^2 = 3.0 for 12G5 using the bivalent model with R_{max} = 88) but not with a 1:1 interaction (χ^2 = 36 for the same data analyzed by the 1:1 model). These results are consistent with each 12G5 antibody binding two CXCR4 receptors on the MLV particle. Similar fitting results were obtained with CTC8 (Fig. 2*F*) and other anti-CCR5 and anti-CXCR4 antibodies (not shown). Because antibody binding to the chemokine receptors was bivalent, this will result in a higher apparent affinity, and the kinetics cannot be described with a simple interaction model. Thus, to accurately measure antibody–receptor binding constants using this technique, Fab fragments will have to be used (24).

Binding Studies of HIV-1 gp120 to MLV Pseudotypes. Direct binding of X4 gp120 proteins to CXCR4 has been difficult to measure (4). In addition, although binding of gp120 subunits derived from R5X4 virus strains to CD4 can be easily detected, binding of these proteins to CCR5, CXCR4, or other coreceptors cannot, perhaps due to low affinity interactions (4–6). We reasoned that the real-time nature of the biosensor would make it possible to measure gp120–CXCR4 interactions more readily than traditional binding methods that rely on steady-state measurements. To simplify the binding interaction, we used a gp120 from a CD4-independent strain of HIV-1 termed 8x, which interacts directly with CXCR4 (9). Initial attempts to measure specific 8x gp120 binding to MLV–CXCR4 on a C1 chip in PBS running buffer were unsuccessful due to nonspecific binding associated with this highly glycosylated protein to the control surface. When the running buffer was changed from PBS to DMEM with 0.1% Pluronic F127, a surfactant previously shown to decrease the nonspecific binding of proteins to gold surfaces (25), we were able to observe specific binding of 8x to MLV–CXCR4 compared with MLV–pCDNA3 (Fig. 4*A*). Binding of 8x could be prevented by the 17b antibody, which binds to the coreceptor binding site in gp120 (11), confirming the specificity of this interaction (Fig. 4*B*). Similar results were obtained when binding studies were performed with 8x in PBS running buffer without Pluronic F127 on an F1 chip, which reduced, but did not completely eliminate, the nonspecific binding of Env (not shown). Regeneration conditions (pH 5/chaotropic solution) used to remove 12G5 and other anti-CXCR4 antibodies also proved to be successful for stripping gp120 from MLV–CXCR4 (Fig. 4*A*). Multiple binding and regeneration cycles of 8x indicated that there was approximately a 2% loss in subtracted signal with each Env binding interaction (not shown). This may be related to inactivation of CXCR4 conformations involved in Env binding or incomplete removal of Env from the sensor surface following regeneration. When dose-response experiments with 8x gp120 were performed (Fig. 4*C*), we calculated the equilibrium dissociation constant to be 506 ± 101 nM (from five independent experiments). The fast off-rate exhibited by 8x gp120 helps explain the difficulty we have experienced in measuring this interaction using standard equilibrium cell-surface binding assays, as all or most of the gp120 dissociates from CXCR4 by the time the washing steps are complete.

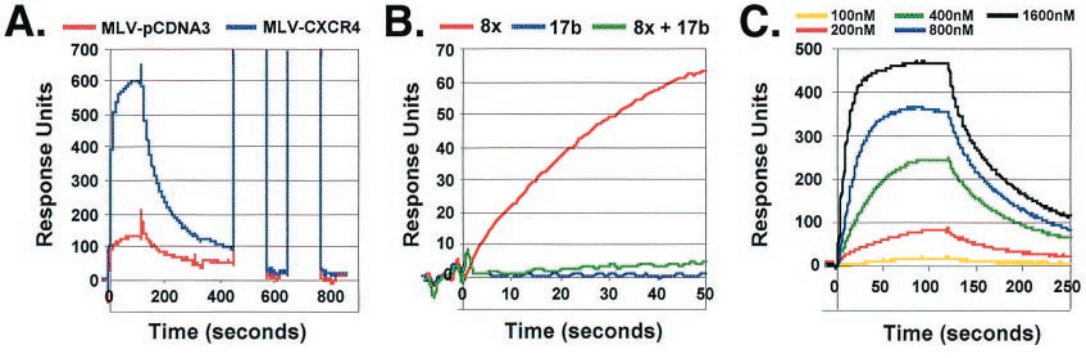

Fig. 4. HIV-1 gp120 binding to MLV–CXCR4. (*A*) Equivalent amounts of MLV–pCDNA3 and MLV–CXCR4 were attached to a Biacore C1 chip, and the binding of 400 nM 8x gp120 was measured to both surfaces in a running buffer of DMEM with 0.1% Pluronic F127. Binding was measured for 120 s and dissociation for 300 s. Two brief regeneration pulses with pH 9/NaCl were used to strip gp120 from the surface. The signal from the pCDNA3 control surface was subtracted in *B* and *C*. (*B*) The ability of mAb 17b, which binds to the conserved coreceptor binding site in Env, to block 8x binding to CXCR4 was measured. Subtracted data for the association phase of 150 nM 8x to MLV–CXCR4 and MLV–pCDNA3 are shown (8x). Association of 750 nM 17b alone and 150 nM 8x prebound to 750 nM 17b is also shown. These experiments were performed using a Biacore F1 chip in PBS running buffer. Regeneration was achieved as in Fig. 1*A*. (*C*) Subtracted data for binding of serial dilutions of 8x gp120 to MLV–CXCR4 and MLV–pCDNA3 are shown.

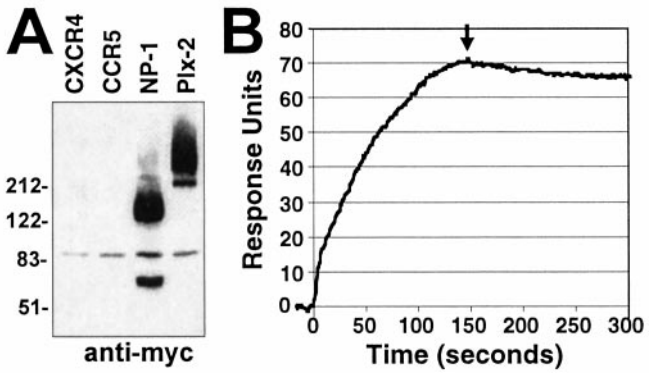

Fig. 5. Binding of collapsin-1 to MLV–NP-1 pseudotypes. (*A*) MLV–NP-1, MLV–Plx-2, MLV–CCR5, and MLV–CXCR4 preparations were blotted with an antibody against the myc epitope, which was present on the C terminus of the NP-1 and Plx-2 constructs. Equivalent amounts of MLV gag were present in these samples (not shown). (*B*) Equivalent amounts of MLV–CCR5 and MLV–NP-1 were attached to a Biacore C1 chip, and binding of 200 nM collapsin-1 was measured to both surfaces in PBS running buffer. The sensorgram shows the MLV–CCR5 signal subtracted from the MLV–NP-1 surface. Collapsin-1 was injected for 150 s, and the arrow indicates the beginning of the wash step. A brief pulse with 2 M $MgCl_2$ was sufficient to regenerate the surface following binding.

Finally, we were able to detect specific binding of a CD4-dependent gp120 from the HXB strain of HIV-1 to MLV–CXCR4, but only when soluble CD4 was included in the running buffer (not shown) so as to trigger the conformational changes in gp120 needed for coreceptor binding.

Binding Studies with Other Membrane Proteins. Having established retroviral pseudotyping as a way to study binding interactions with antibodies and HIV-1 gp120 with chemokine receptors using the optical biosensor, we determined whether binding to other membrane proteins could be measured with this technique. Neuropilin-1 (NP-1) is a member of a related group of type 1 membrane proteins involved in axonal guidance in the developing nervous system. A family of protein ligands, termed collapsins, binds to NP-1 receptors on axons and triggers axonal repulsion and redirection (26). After determining that NP-1 and a similar protein, plexin-2, could be incorporated into MLV particles (Fig. 5*A*), we attached MLV–NP-1 to a biosensor surface and measured binding of collapsin-1. As shown in Fig. 5*B*, collapsin-1 specifically interacted with MLV–NP-1. These results indicate that a diverse group of membrane proteins can be incorporated and presented in MLV particles for binding studies in the optical biosensor.

Discussion

Optical biosensor technology can be used to study molecular interactions in real time, making it possible to accurately measure kinetic and equilibrium binding constants (7, 8). Whereas interactions between soluble molecules can be routinely measured, it has not been possible to present membrane proteins in their native, lipid environments on the sensor surface for a number of technical reasons. These problems can sometimes be circumvented by generating soluble ectodomain fragments of type I and type II integral membrane proteins, but proteins that span the membrane multiple times or that exist as multimeric complexes are not as easily manipulated. In principle, integral membrane proteins can be purified and reconstituted into artificial membranes that can be attached to the sensor surface. However, purification and reconstitution of membrane proteins is a laborious and empirically driven process, and thus far it has not been used successfully in an optical biosensor format with the exception of bacterial rhodopsin (27). As a result, entire classes of membrane proteins, such as seven transmembrane domain receptors, have not been studied using this technique. In the case of HIV, there are many instances in which standard equilibrium binding assays are not sufficiently sensitive to study in detail, or sometimes even detect, interactions between the viral Env protein and its 7TM coreceptors (4–6). Because HIV–coreceptor interactions are critically important determinants of viral tropism and pathogenesis, and because these receptors are important drug targets (1), this is a significant shortcoming. Therefore, we took advantage of the fact that retroviruses can incorporate cellular membrane proteins into their lipid envelopes during the process of budding from the cell surface. In effect, we have used retroviral pseudotypes as model membrane vesicles that, due to the presence of the viral core, are homogeneous in size, easily purified, and stable. In addition, incorporation of a membrane protein into a retrovirus avoids the need for detergent solubilization, purification, and reconstitution. Although not all cellular membrane proteins can be incorporated into retroviral envelopes, a significant number can, indicating that the approach described here should be broadly applicable.

A host of type I, type II, and multiple membrane-spanning cellular membrane proteins have been shown to be incorporated into retrovirus particles, including class I and class II MHC proteins, CD4, various ICAMs, a tetraspan protein (CD63), as well as multiple membrane-spanning proteins such as the murine cationic amino acid transporter, which functions as a receptor for the ecotropic murine leukemia virus (ref. 20 and references therein). For this approach to work in the optical biosensor format, the incorporated membrane proteins must retain their native conformation. Studies in which viral receptors are incorporated into retroviral particles, enabling these particles to infect cells expressing the cognate viral Env glycoproteins, demonstrate this. For example, incorporation of CD4 and either CCR5 or CXCR4 into virus particles enables these virions to infect cells expressing R5 or X4 HIV-1 Env proteins, respectively (28, 29). Because the determinants on CD4 and CCR5 recognized by the viral Env protein are conformationally complex (30), these results indicate that the pseudotyped receptors retain their native conformation. In addition, this shows that at least two different proteins can be incorporated into a given virus particle; it also shows that because membrane fusion is a cooperative process requiring multiple receptor binding events (31), multiple copies of each can be incorporated. In the case of HIV-1, it is estimated that six CCR5 molecules are needed to support membrane fusion (32) and that multiple CD4 molecules are also needed (33). Our results support these conclusions; the 7TM and type I membrane proteins studied here retained their native conformations as judged by their abilities to bind a variety of conformationally sensitive ligands. The presence of bivalent interactions also suggests that there is lateral mobility in the retroviral membrane, providing further evidence that they are a good cell-surface surrogate.

The efficiency with which a protein can be pseudotyped into a virus particle can be influenced by the location and degree of expression and the nature of the cytoplasmic domain of the protein (19, 21, 34). A prerequisite for pseudotype formation with MLV is that the protein of interest be expressed on the cell surface. Potentially, viruses that bud from intracellular compartments could be used to incorporate cellular membranes that reside elsewhere in the cell, although we have not investigated this approach. Alternatively, proteins retained in intracellular organelles could be retargeted to the cell surface and incorporated into MLV particles by modifying retention or targeting motifs. There is increasing evidence that some viruses selectively bud from the cell surface through detergent-insoluble lipid rafts (35, 36). Therefore, targeting proteins of interest to lipid rafts

could, for some virus types, improve pseudotype formation. Once the protein is expressed at the proper location on the cell surface, incorporation efficiency is likely to be related to expression levels. Because high level expression is desirable, we used a transient expression system using a cell type that is easily transfectable as well as being capable of high levels of protein production. In excess of 100,000 CCR5 and CXCR4 molecules are expressed per cell using this approach (12). Pseudotype formation may in some cases be improved by constructing chimeric molecules in which the cytoplasmic domain of a membrane protein is replaced with that of the retroviral Env protein. Shortening a long cytoplasmic region may also improve incorporation into viral pseudotypes by reducing negative interactions between bulky cytoplasmic domains and retroviral gag protein (34). A final factor to consider is the type of virus used. In addition to MLV, other viruses such as vesicular stomatitis virus and HIV can also be used to generate pseudotypes, providing additional options for packaging cellular membrane proteins into virus particles (28, 29).

The use of retroviral pseudotypes as membrane presentation vehicles will make it possible to study ligand interactions with many different cellular membrane proteins using optical biosensors. This approach has interesting implications for drug discovery in which binding of small molecules to 7TM and other membrane receptors could be measured. In our study, attachment of 4,000 to 6,000 RUs of virus particles enabled us to obtain up to several hundred RUs of specific antibody binding. This is considerably in excess of what is needed to obtain accurate kinetic measurements, as accurate responses can be measured well below 100 RU, and even below 10 RU in some cases (24). It has already been demonstrated that it is possible to detect binding of low mass compounds using an optical biosensor (37, 38). Because the signal measured by the optical biosensor is proportional to mass, it is likely that improved attachment of retroviral pseudotypes will be needed to measure binding of small molecular weight compounds. Attachment of larger amounts of pseudotypes should be possible because we endeavored to keep the binding capacity of our surfaces low so as to minimize mass transport effects that could be associated with the high molecular weight ligands that we used (24). The ability to measure binding of small molecules to membrane receptors with an optical biosensor could make this a useful secondary screening tool. Advantages of this approach include the fact that only a small amount of sample is needed and that the ligand does not have to be labeled. The ability of many compounds to bind a given receptor could be rapidly screened, making it possible to identify compounds with desirable association and dissociation kinetics, information not normally available from other screening methods. In the case of HIV-1, this approach should make it possible to directly measure some Env–receptor interactions, providing information on the relationship between Env–receptor affinity and viral tropism and pathogenesis, and also on how small molecule inhibitors interact with the major HIV coreceptors and block Env binding and viral infection.

We thank Biacore AB (Uppsala, Sweden) for use of a Bia 2000, making it possible to complete these studies. Aimee Edinger, Jonathan Raper, Irwin Chaiken, Mike Malim, Paul Bates, and their laboratories provided helpful advice and reagents. We also appreciate the helpful discussions and biosensor instrument time provided by Gary Cohen, Roz Eisenberg, and Ann Rux, and technical help provided by Ann Dude. Giant Truck Stop in Gallup, NM provided critical assistance in information transfer for T.L.H., who was supported by National Institutes of Health Grant T32 AI07325 and by a Pine Family Foundation Fellowship. R.W.D. was supported by National Institutes of Health Grant R01 40880, by an Elizabeth Glaser Scientist Award from the Pediatric AIDS Foundation, and by a Burroughs Wellcome Fund Translational Research Award.

1. Berger, E. A., Murphy, P. M. & Farber, J. M. (1999) *Annu. Rev. Immunol.* **17,** 657–700.
2. Doranz, B. J., Baik, S. S. W. & Doms, R. W. (1999) *J. Virol.* **73,** 10346–10358.
3. Wu, L., Gerard, N. P., Wyatt, R., Choe, H., Parolin, C., Ruffing, N., Borsetti, A., Cardoso, A. A., Desjardin, E., Newman, W., Gerard, C. & Sodroski, J. (1996) *Nature (London)* **384,** 179–183.
4. Doranz, B. J., Orsini, M. J., Turner, J. D., Hoffman, T. L., Berson, J. F., Lu, Z.-H., Hoxie, J. A., Peiper, S. C., Brass, L. F. & Doms, R. W. (1999) *J. Virol.* **73,** 2752–2761.
5. Baik, S., Doms, R. W. & Doranz, B. J. (1999) *Virology* **259,** 267–273.
6. Etemad-Moghadam, B., Sun, Y., Nicholson, E. K., Fernandes, M., Liou, K., Gomila, R., Lee, J. & Sodroski, J. (2000) *J. Virol.* **74,** 4433–4440.
7. Canziani, G., Zhang, W., Cines, D., Rux, A., Willis, S., Cohen, G., Eisenberg, R. & Chaiken, I. (1999) *Methods* **19,** 253–269.
8. Rich, R. L. & Myska, D. G. (2000) *Curr. Opin. Biotechnol.* **11,** 54–61.
9. Hoffman, T. L., LaBranche, C., Zhang, W., Canziani, G., Robinson, J., Chaiken, I., Hoxie, J. A. & Doms, R. W. (1999) *Proc. Natl. Acad. Sci. USA* **96,** 6359–6364.
10. Thali, M., Moore, J., Furman, C., Charles, M., Ho, D., Robinson, J. & Sodroski, J. (1993) *J. Virol.* **67,** 3978–3988.
11. Kwong, P. D., Wyatt, R., Robinson, J., Sweet, R. W., Sodroski, J. & Hendrickson, W. A. (1998) *Nature (London)* **393,** 648–659.
12. Lee, B., Sharron, M., Blanpain, C., Doranz, B. J., Vakili, J., Setoh, P., Berg, E., Liu, G., Guy, H. R., Durell, S. R., *et al*. (1999) *J. Biol. Chem.* **274,** 9617–9626.
13. Chabot, D. J., Chen, H., Dimitrov, D. S. & Broder, C. C. (2000) *J. Virol.* **74,** 4404–4413.
14. Endres, M. J., Clapham, P. R., Marsh, M., Ahuja, M., Turner, J. D., McKnight, A., Thomas, J. F., Stoebenau-Haggarty, B., Choe, S., Vance, P. J., *et al*. (1996) *Cell* **87,** 745–756.
15. Doranz, B. J., Grovit-Ferbas, K., Sharron, M. P., Mao, S. H., Goetz, M. B., Daar, E. S., Doms, R. W. & O'Brien, W. A. (1997) *J. Exp. Med.* **186,** 1395–1400.
16. Evan, G. I., Lewis, G. K., Ramsay, G. & Bishop, J. M. (1985) *Mol. Cell. Biol.* **5,** 3610–3616.
17. Koppel, A. M., Feiner, L., Kobayashi, H. & Raper, J. A. (1997) *Neuron* **19,** 531–537.
18. Andersson, K., Hämäläinen, M. & Malmqvist, M. (1999) *Anal. Chem.* **71,** 2475–2481.
19. Young, J. A., Bates, P., Willert, K. & Varmus, H. E. (1990) *Science* **250,** 1421–1423.
20. Balliet, J. W. & Bates, P. (1998) *J. Virol.* **72,** 671–676.
21. Suomalainen, M. & Garoff, H. (1994) *J. Virol.* **68,** 4879–4889.
22. Myszka, D. G. (1999) *J. Mol. Recognit.* **12,** 390–408.
23. Brelot, A., Heveker, N., Pleskoff, O., Sol, N. & Alizon, M. (1997) *J. Virol.* **71,** 4744–4751.
24. Myszka, D. G. (1999) *J. Mol. Recognit.* **12,** 279–284.
25. Green, R. J., Davies, M. C., Roberts, C. J. & Tendler, S. J. B. (1998) *J. Biomed. Mater. Res.* **42,** 165–171.
26. He, Z. & Tessier-Lavigne, M. (1997) *Cell* **90,** 739–751.
27. Salamon, Z., Wang, Y., Brown, M. F., Macleod, H. A. & Tollin, G. (1994) *Biochemistry* **33,** 13706–13711.
28. Endres, M. J., Jaffer, S., Haggarty, B., Turner, J. D., Doranz, B. J., O'Brien, P. J., Kolson, D. L. & Hoxie, J. A. (1997) *Science* **278,** 1462–1464.
29. Schnell, M. J., Johnson, J. E., Buonocore, L. & Rose, J. K. (1997) *Cell* **90,** 849–857.
30. Hoffman, T. L. & Doms, R. W. (1998) *AIDS* **12,** Suppl. A, S17–S26.
31. Hernandez, L. D., Hoffman, L. R., Wolfsberg, T. G. & White, J. M. (1996) *Annu. Rev. Cell Dev. Biol.* **12,** 627–661.
32. Kuhmann, S. E., Platt, E. J., Kozak, S. L. & Kabat, D. (2000) *J. Virol.* **74,** 7005–7015.
33. Layne, S. P., Merges, M. J., Dembo, M. B., Spouge, J. L. & Nara, P. L. (1990) *Nature (London)* **346,** 277–279.
34. Henriksson, P., Pfeiffer, T., Zentgraf, H., Alke, A. & Bosch, V. (2000) *J. Virol.* **73,** 9294–9302.
35. Nguyen, D. H. & Hildreth, J. E. K. (2000) *J. Virol.* **74,** 3264–3272.
36. Zhang, J., Pekosz, A. & Lamb, R. A. (2000) *J. Virol.* **74,** 4634–4644.
37. Markgren, P.-O., Hämäläinen, M. & Danielson, U. (1999) *Anal. Biochem.* **265,** 340–350.
38. Strandh, M., Persson, B., Roos, H. & Ohlson, S. (1998) *J. Mol. Recognit.* **11,** 188–190.